

The 1.4 GHz and $H\alpha$ Luminosity Functions and Star Formation Rates from Faint Radio Galaxies

B. Mobasher¹, L. Cram², A. Georgakakis¹ and A. Hopkins²

¹*Astrophysics Group, Blackett Laboratory, Imperial College, Prince Consort Rd, London SW7 2BZ, UK*

²*School of Physics, University of Sydney, Sydney NSW 2006, Australia*

10 April 2018

ABSTRACT

A sample of over 1000 objects selected from a 1.4 GHz survey made by the Australia Telescope Compact Array (ATCA) is used to study the properties of the faint radio source population. The sample, covering an area of ≈ 3 deg², is 50% complete to 0.2 mJy. Over 50% of the radio sources are found to have optical counterparts brighter than $R \approx 21.5$. Spectroscopic observations of 249 optically identified radio sources have been made, using the 2-degree Field (2dF) facility at the Anglo-Australian Telescope (AAT). Redshifts and equivalent widths of several spectral features (e.g., $H\alpha$ and [OII] λ 3727) sensitive to star formation have been measured. On the basis of the photometric and spectroscopic data, the optically identified radio sources are classified as (i) absorption-line galaxies, (ii) star-forming galaxies and (iii) Seyfert-like galaxies.

The spectroscopic sample is corrected for incompleteness and used to estimate the 1.4 GHz and $H\alpha$ luminosity functions (LFs) and luminosity density distributions. The 1.4 GHz LF of the star-forming population has a much steeper faint-end slope (1.85) than the ellipticals (1.35). This implies an increasing preponderance of star-forming galaxies among the optically identified (i.e., $z \lesssim 1$) radio sources at fainter flux densities. The $H\alpha$ LF of the faint radio population agrees with published $H\alpha$ LFs derived from local samples selected by $H\alpha$ emission. This suggests that the star-forming faint radio population is coincident with the $H\alpha$ selected population.

The 1.4 GHz and $H\alpha$ luminosity densities have been used to estimate the

star formation rates (SFRs). The two SFRs agree, both giving a SFR density of $0.032 \text{ M}_{\odot} \text{ yr}^{-1} \text{ Mpc}^{-3}$ in the range $z \lesssim 1$. Radio selection appears to be as effective as $\text{H}\alpha$ selection in finding the galaxies which dominate star formation at a given epoch. Although the sample contains many galaxies lying beyond $z \approx 0.3$, it does not reveal a significant rise in the global star formation rate with increasing redshift. This result suggests that the optical counterparts of galaxies undergoing vigorous star formation at redshifts beyond $z \approx 0.3$ are generally fainter than $R \approx 21$.

Key words: cosmology: observations - galaxies: starburst - galaxies: starburst - radio continuum: galaxies

1 INTRODUCTION

The population of apparently bright radio sources ($S_{1.4} \gtrsim 100 \text{ mJy}$) is dominated by *classical radio galaxies*, whose optical hosts, when detectable, are usually identified as luminous elliptical galaxies with red colours and absorption-line optical spectra, although some are hosted by QSOs. The elliptical hosts sometimes emit nebular emission lines, which can be quite strong for the most luminous radio sources (Hine & Longair 1979). The lines appear to be excited by an active galactic nucleus (AGN) radiating a non-stellar continuum (Baum & Heckman 1989). The normalised source count distribution of the classical radio galaxies falls sharply with decreasing flux density, as a result of cosmological dimming and strong source evolution for $z \lesssim 2$ (Wall & Jackson 1997).

The apparently bright radio source population contains, in addition to these classical radio galaxies, a small proportion of spiral/irregular galaxies. These are markedly different from the classical radio galaxies. For example, even samples selected to have large radio-to-optical luminosity ratios have a radio luminosity smaller than that of most classical radio galaxies (Condon et al. 1982). The core/jet/lobe radio morphology of classical radio galaxies is absent, and replaced by centrally concentrated but nevertheless diffuse emission. Moreover, a high proportion of radio-bright spirals have peculiar optical morphologies and strong emission lines excited by stellar photospheric radiation, apparently reflecting an enhanced rate of star formation (Condon et al. 1982).

Spiral/irregular galaxies do not contribute in significant numbers to radio source counts for $S_{1.4} \gtrsim 10 \text{ mJy}$. However, radio surveys reaching fainter flux density limits, $S_{1.4} \lesssim 1 \text{ mJy}$, reveal a significant change in the slope of the normalised source count distribution at

$S_{1.4} \approx 5$ mJy [Windhort, van Heerde & Katgert (1984); Condon (1984); Fomalont et al. (1984); Mitchell & Condon (1985); Windhorst et al. (1985)]. The change suggests the possible existence of a numerous population of apparently faint radio sources unlike the classical radio galaxies. Optical photometry and spectroscopy of the population reveals that many of the faint radio sources are associated with blue galaxies often exhibiting peculiar (compact, interacting and merging) morphologies. Kron, Koo & Windhorst (1985) and Thuan & Condon (1987) have shown that these galaxies are quite unlike the hosts of classical radio galaxies, but are reminiscent of radio-bright local spiral galaxies.

The central astrophysical importance of the faint radio population lies in the fact that the unevolving, local luminosity function of the non-AGN radio source population can explain neither the large number counts nor the source-count distribution at sub-mJy flux densities (Condon 1984). Attempts to resolve this problem show that significant evolution may have occurred over the redshift range spanned by the observed population. For example, Danese et al. (1987) established consistency by adopting a model which includes luminosity evolution of a starburst/interacting population over an e -folding time of about 25% of the Hubble time. There are hints that the IRAS galaxy population undergoes similar evolution, although the IRAS surveys did not extend to the faint levels corresponding to deep radio surveys (Lonsdale et al. 1987). Population evolution of FIR-selected galaxies has been confirmed by deeper FIR observations made by the *Infrared Space Observatory (ISO)* (Rowan-Robinson et al. 1997). Additional evidence, consistent with the hypothesis of recent ($z \lesssim 1$) rapid evolution of a large fraction of the faint radio population, has come from the improved redshift distribution statistics for the optical counterparts of faint radio sources reported by Benn et al. (1993) and Hopkins et al. (1999).

The cosmological significance of this evolving population has been clarified by optical/UV studies using deep ground-based observations and data from the *Hubble Space Telescope (HST)*. Studies by Madau et al. (1996) imply not only that the space density of star-forming, morphologically disturbed galaxies increases with redshift to $z \gtrsim 1$, but also that this increase is associated with a corresponding increase in the global star formation rate in the Universe. A similar picture emerges from observations of faint sub-mm sources (Blain et al. 1998).

The 1.4 GHz luminosity of a spiral/irregular galaxy can be used to estimate its star formation rate (SFR), assuming the appropriate calibration (Condon & Yin 1990; Condon 1992). Using this result and published 1.4 GHz luminosity functions, Cram (1998) has argued

that the global rate of star formation appears to be dominated by galaxies with $SFR \gtrsim 15 M_{\odot} \text{ yr}^{-1}$. This implies that galaxies with $P_{1.4} \gtrsim 5 \times 10^{22} \text{ W Hz}^{-1}$ are likely to dominate the global SFR . Such a galaxy would be brighter than $10 \mu\text{Jy}$ at $z = 1$, implying that deep radio surveys probe the population which dominates global star formation to cosmologically significant redshifts.

The discoveries summarised above suggest that the faint radio source population may well contain *all* of the galaxies which dominate the global star-formation processes revealed by optical/UV diagnostics, at least for redshifts out to $z \approx 1$ at the current limits of radio surveys. However, the implications of this have been explored directly for only a few dozen objects [Benn et al. (1993); Hammer et al. (1995)]. In the present study, we use a sample of over 420 faint, radio-selected galaxies with optical data to define a well characterised sub-sample of star-forming objects, many (over 50%) with measured redshifts. From this sub-sample, we use the radio and $\text{H}\alpha$ luminosities to estimate luminosity functions, luminosity densities and star-formation rates in the era $z \lesssim 1$. We show that the radio and optical properties of this sample are consistent with one another, and with the properties of samples from the *local* Universe. We use the results to provide an unbiased estimate of the star-formation history (free from dust effects) in the surveyed volume.

In the following section we summarise the observations. Section 3 presents the luminosity functions and star formation rates, and Section 4 discusses the results from this investigation.

2 OBSERVATIONS

The observations have been accumulated during several campaigns connected with the Phoenix Deep Survey. The criteria used to select the field, as well as the radio observations and data reduction methods, are discussed by Hopkins et al. (1998). The radio observations were made with the Australia Telescope Compact Array (ATCA) at 1.4 GHz, covering an area of diameter 2° , centered at $\text{RA}(2000) = 01^{\text{h}} 14^{\text{m}} 12^{\text{s}}.16$; $\text{Dec.}(2000) = -45^{\circ} 44' 8''.0$. A total of 1079 radio sources are detected to $S_{1.4} \approx 0.1 \text{ mJy}$. The radio flux distribution for the entire survey is presented in Fig. 1 (solid line). The survey is 60% complete to $S_{1.4} \approx 0.3 \text{ mJy}$, with a total of 804 sources detected to this flux limit. The completeness drops to 50% at $S_{1.4} \approx 0.2 \text{ mJy}$, with a total of 964 galaxies to this limit. The 80% completeness limit is achieved at about $S_{1.4} = 0.4 \text{ mJy}$ with 656 galaxies detected. In the present study, we con-

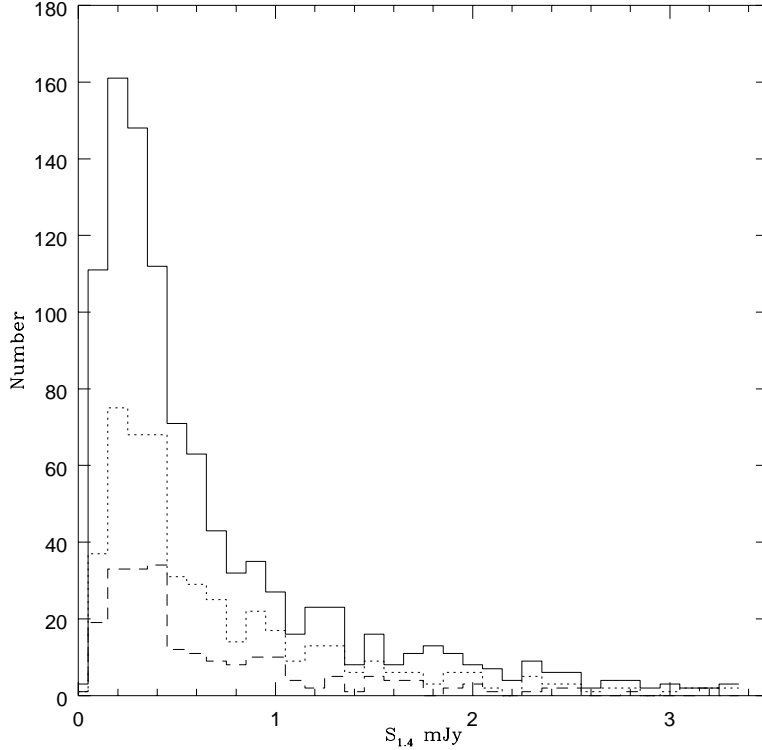


Figure 1. 1.4 GHz radio flux distribution of detected radio sources (solid line), radio sources with optical identifications (dotted line) and radio sources with spectroscopic measurements (dashed line).

sider galaxies with $S_{1.4} > 0.2$ mJy and refer to this in the following sections as the ‘complete’ radio sample.

CCD observations of the entire radio survey area were attempted in the V and R -bands, using the Anglo-Australian Telescope (AAT). The observations were performed to a magnitude limit of $R = 22.5$, corresponding to the limit expected for successful spectroscopy with the two-degree field facility (2dF) of the AAT. Over 50% of the radio sources have optical identifications, corresponding to a total of 420 galaxies to $S_{1.4} \approx 0.3$ mJy and 490 galaxies to 0.2 mJy. The radio flux distribution for galaxies with optical IDs is shown in Fig. 1 (dotted line). The optical photometry and radio-optical source identifications are described in Georgakakis et al. (1998).

Spectroscopic observations were carried out for a random sample of the optically identified radio galaxies to a limiting magnitude of $R = 21.5$, using the 2dF facility. Accurate redshifts were successfully measured for a total of 228 radio sources, using several lines, including $H\beta$, $H\alpha$, $[\text{OII}]\lambda 3727$ and $[\text{OIII}]\lambda 5003$ (Georgakakis et al. 1998). Of this number, 210 galaxies are in the ‘complete’ radio survey (i.e., have $S_{1.4} > 0.2$ mJy), implying $\approx 50\%$

completeness for the spectroscopic sample used here. The fraction of galaxies with spectroscopic data at any given radio flux is presented in Fig. 1 (dashed line). Diagnostic spectral line ratios were estimated from these spectra and used to classify the galaxies in the spectroscopic sample. This is explained in detail in Georgakakis et al. (1998) where the galaxies are classified as (i) elliptical, (ii) starforming, (iii) Seyfert and (iv) a small number of objects for which the spectral quality was not high enough to allow an accurate classification. Examples of the 2dF spectra of the radio sources classified to the above four sub-types are shown in Fig. 2.

Spectroscopic signatures of probable star formation (mainly [OII] λ 3727 and H α) are detected in the spectra of 63% of the faint radio sources. The redshift distributions for the complete radio sample ($S_{1.4} > 0.2$ mJy) is compared in Fig. 3 with that of the sub-sample showing evidence of star formation activities as revealed from their spectra. The majority of star-forming radio sources brighter than the optical magnitude limit of this survey have $z \lesssim 0.3$.

One aim of this study is to derive quantitative optical measures of the star formation rate, using H α wherever possible, to compare with the results from the radio data. However, an absolute flux calibration is not available for our 2dF spectra. Thus, the H α luminosity ($P_{H\alpha}$) of each galaxy has been estimated from its measured H α equivalent width, EW_{α} , and the R -band magnitude. The spectral synthesis models of Bruzual and Charlot (1993) were then used to estimate the R -band K -corrections and the rest-frame continuum luminosity at H α , C_{α} (Georgakakis et al. 1998). The H α luminosity is then estimated using

$$P_{H\alpha} = C_{\alpha} \times EW_{H\alpha}.$$

For the few galaxies with $z > 0.3$, H α shifts out of the observed spectral range. For these, we used [OII] λ 3727 as a proxy for H α , converting its equivalent width using the relation (Kennicutt 1992)

$$EW_{OII} = 0.4 \times EW_{H\alpha}.$$

As noted by Kennicutt (1992), the scatter about this correlation has an RMS dispersion of about 50%, due in part to galaxy-to-galaxy differences in extinction.

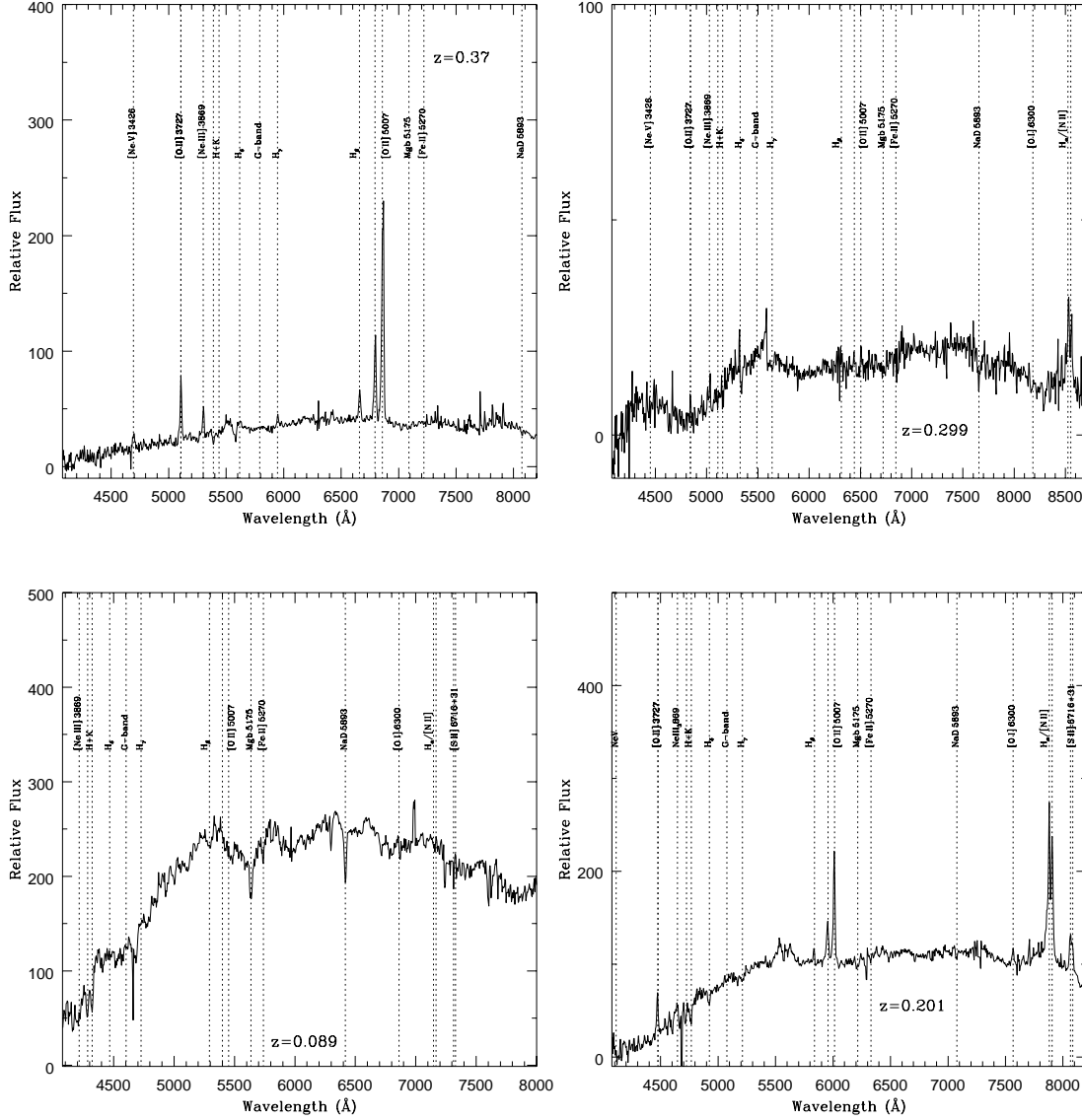


Figure 2. 2dF spectra for the 4 types of galaxies classified here. The identified spectral lines are marked with the estimated redshift of the objects specified. The spectra correspond to; Elliptical (bottom left), Star-forming (top left), Seyfert 2 (bottom right) and ‘unclassified’ (top right)

3 LUMINOSITY FUNCTIONS AND STAR FORMATION RATES

In this section we estimate the 1.4 GHz and $H\alpha$ luminosity functions for our sample. These will then be used to determine the luminosity density distribution and, for the star-forming galaxies, the star formation rate. To ensure an adequate sample size, we first assume that the sample statistics are independent of redshift (i.e. that there is no dependence of the selection functions on redshift). We consider two radio samples, consisting of the elliptical and the star-forming populations, as classified from their optical spectra (the small proportion of

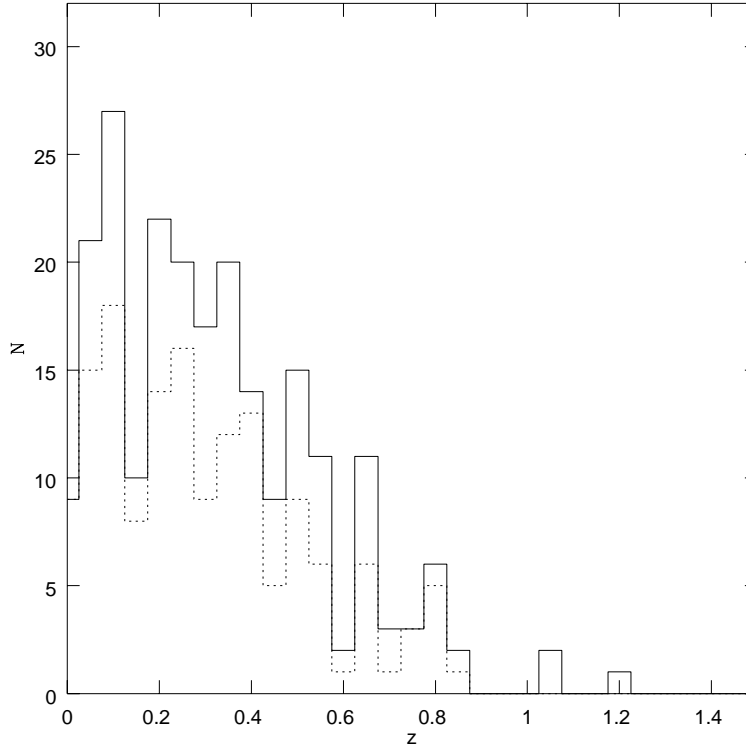


Figure 3. The redshift distribution (solid line) of the Phoenix sample compared with the distribution of galaxies with H α (or [OII] λ 3727) detections (dotted line).

Seyfert or unclassified galaxies is excluded). Our H α sample combines all galaxies in the radio-selected sample which exhibit H α emission, since this would appear to provide a sample selected in much the same way as the objective prism sample of Gallego et al. (1995).

3.1 Sample completeness and selection effects

There are two sources of incompleteness in the present spectroscopic survey. Firstly, only radio sources with optical counterparts have been observed spectroscopically. This biases the spectroscopic sample against optically faint galaxies (e.g., distant, dusty and/or low surface brightness objects). Secondly, only a randomly selected sub-sample of the optically identified galaxies which satisfy the optical magnitude range accessible by the 2dF have been observed spectroscopically.

To correct for the first bias we define a completeness function at any given radio flux density, η_1 ($S_{1.4}$), as the ratio of the number of radio sources with optical identifications to the total number of sources in the complete radio survey. This completeness function is displayed in Fig. 4a. The second bias can be corrected using a completeness function at

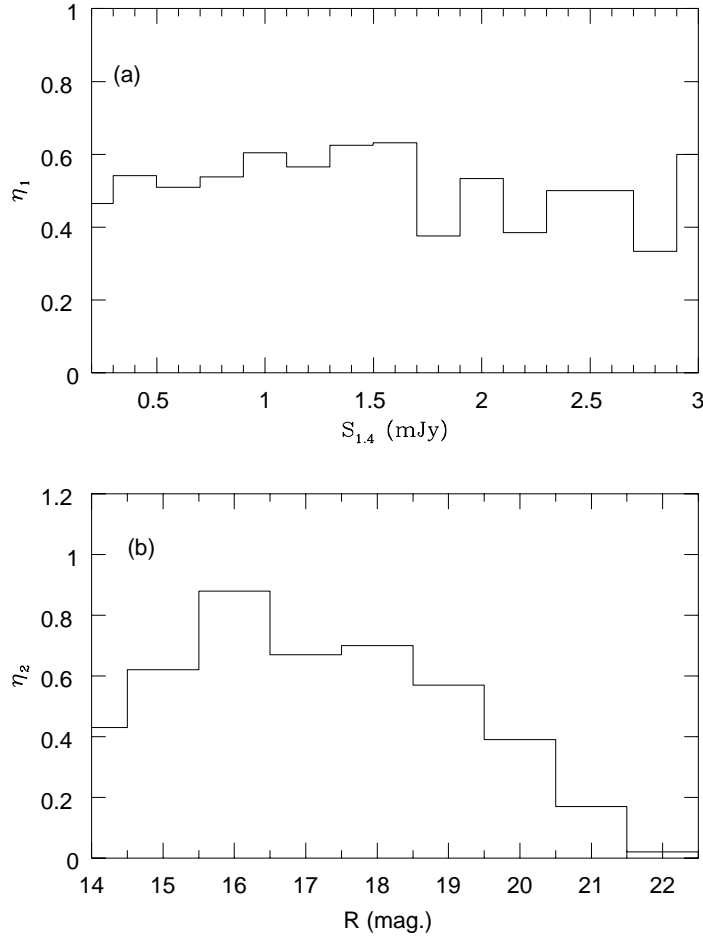


Figure 4. (a) The selection function $\eta_1(S_{1.4})$ defined as the ratio of the number of faint radio sources with optical identifications to the total number of radio sources in the complete radio survey. (b) The selection function $\eta_2(R)$ defined as the ratio of the number of galaxies with measured spectra to the total number of sources with optical counterparts in the complete radio survey.

any given optical magnitude, $\eta_2(R)$, defined as the ratio of the number of galaxies with measured spectra, to the total number of sources with optical counterparts in the ‘complete’ radio survey ($S_{1.4} > 0.2$ mJy). This completeness function is shown in Fig. 4b. The final completeness function is then $p_1(S_{1.4}, R) = \eta_1(S_{1.4}) \eta_2(R)$.

The H α sample systematically excludes optically identified but faint galaxies which yield spectra with low S/N ratios and hence no reliable detection of H α (or [OII] λ 3727). A completeness function to correct for this selection effect, $p_2(R)$, will depend on the optical magnitude of an identification, and is defined as the ratio of the number of objects with H α detection to the total number of sources with optical identifications in the complete radio survey. The function $p_2(R)$ is shown in Fig. 4c.

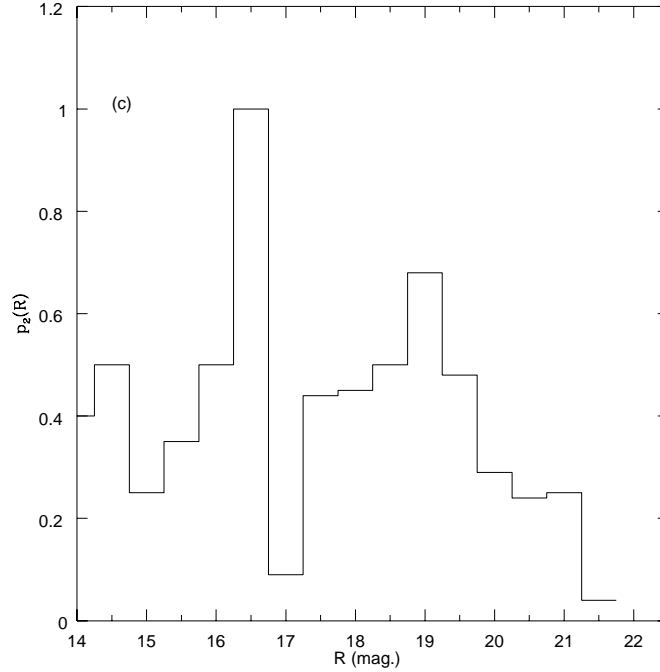


Figure 4. (c) The selection function of the H α survey, $p_2(R)$, defined as the ratio of the number of galaxies with H α detected to the total number of galaxies with optical identification.

3.2 The 1.4 GHz and H α luminosity functions

Using the completeness functions derived above, we correct the sample for incompleteness and selection effects and estimate its radio [$\Phi_{1.4}(P_{1.4})$] and H α [$\Phi_\alpha(P_{H\alpha})$] luminosity functions as

$$\Phi_k(P_k) = \Sigma_i \left(\frac{1}{V_{max,i}} \right),$$

where the summation is over the number of galaxies in radio or H α flux bins in the complete sample, with V_{max} given by

$$V_{max} = \frac{\Omega}{4\pi} \frac{c}{H_0} \int_{z_1}^{z_2} \frac{p_k d_L^2}{(1+z)^2 (1+2q_0 z)^{1/2}} dz.$$

Here, p_k is the completeness function corresponding to the radio ($k = 1$) and H α ($k = 2$) surveys, d_L is the luminosity distance, and the integral limits are $z_1 = \max(z_{rad}, z_{opt}, z_{min})$ and $z_2 = \min(z'_{rad}, z'_{opt}, z_{max})$. The quantities z_{rad} and z_{opt} are, respectively, the redshifts corresponding to the bright radio flux and optical R -band magnitude limits of the survey while z'_{rad} and z'_{opt} are the maximum redshifts at which a source could be included (at the flux limit of the survey) in the radio sample and be detected at the optical wavelength. The quantities z_{min} and z_{max} are respectively the minimum and maximum redshifts covered by galaxies in the radio survey. K -corrections are estimated in the R -band using model spectral

energy distributions for intermediate-type spirals (section 2), and at 1.4 GHz assuming an spectral energy distribution proportional to $\nu^{-0.7}$.

A parametric form which successfully models the luminosity functions of the IRAS (Saunders et al. 1990) and faint radio (Rowan-Robinson et al. 1993) sources has been adopted to fit the luminosity functions in this study. It is the function

$$\Phi(P) d(\log P) = C^* \left(\frac{P}{P^*}\right)^{1-\alpha} \exp\left[-\frac{1}{2\sigma^2} \log_{10}^2\left(1 + \frac{P}{P^*}\right)\right] d(\log P),$$

where C^* , P^* , σ and α are the fitted parameters. Fig. 5 displays the radio (1.4 GHz) LF for all the galaxies in the ‘complete’ radio survey (Fig. 5a), the star-forming population (Fig. 5b) and the ellipticals (Fig. 5c). The error bars represent uncertainties assuming Poisson statistics. The $\langle V/V_{max} \rangle$ estimates are given in Table 1. The parametric fits to the radio LFs, assuming the above form, are carried out for cases with no evolution and assuming luminosity evolution in the form $P_{1.4}(z) = P_{1.4}(0) (1+z)^3$. This form of luminosity evolution is adopted to be consistent with recent optical (Lilly et al 1996), far-infrared (Kawara et al 1998) and radio (Rowan-Robinson et al 1993) observations. The fits were performed to the LFs corresponding to all the galaxies in the ‘complete’ radio survey, the starburst population and elliptical galaxies. Figure 5 compares the results for the two cases, assuming no-evolution (solid line) and luminosity evolution (dotted line). The estimated 1.4 GHz LF parameters are listed in Table 1. For a given population of galaxies in Figures 5a, 5b and 5c, we find no significant difference in the radio LFs between the two cases (assuming no evolution or luminosity evolution in the form $(1+z)^3$). This result argues against the presence of significant luminosity evolution in the radio LFs in the redshift range, $0 < z < 1$, covered by the present survey.

The LF for the star-forming radio sources in Fig. 5b is compared with Condon’s (1989) estimates from the bright spirals (open circles), starbursts (filled triangles) and a sample of UGC galaxies with diameter $> 1'$ (asterisks). The present sample has a mean redshift of $\langle z \rangle = 0.3$, compared to $\langle z \rangle = 0.05$ for galaxies from Condon (1989) and Sadler et al (1989). Therefore, the comparison between these samples in Figures 5b and 5c assumes no evolution for the radio sources in the range $0 < z < 0.3$, as justified from the above results. The independently derived LFs show excellent agreement in both shape and normalisation. Moreover, extrapolation of our radio LF in Fig. 5b to faint fluxes ($P_{1.4} < 10^{21}$ W/Hz) agrees well with the faint-end of the radio (1.4 GHz) LF for the spiral and irregular galaxies in Condon (1989). Fig. 5c compares the radio LF derived here with that of the elliptical galaxy

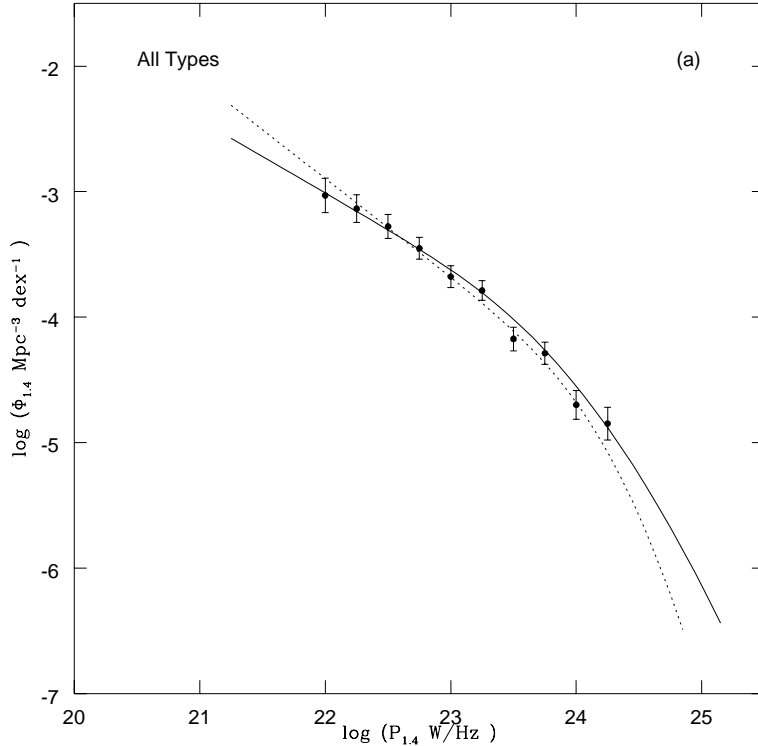


Figure 5. (a) The 1.4 GHz luminosity functions for all galaxies in the ‘complete’ radio survey (filled circles). The sample is corrected for incompleteness. The curve is a parametric fit to the LF, using the function described in the text and assuming no evolution (solid line) and luminosity evolution in the form $(1+z)^3$ (dotted line). The LF is estimated in the range $z < 1$.

radio luminosity function from Sadler, Jenkins & Kotanyi (1989) converted to 1.4 GHz assuming $S_\nu \propto \nu^{-0.7}$. Considering that these samples have different selection criteria, depths and completeness limits, the agreement between the two LFs in Fig. 5c is remarkably good.

The $H\alpha$ LF of the sub-mJy radio sources with $H\alpha$ detection is shown in Figure 6. The error bars are estimated assuming Poisson statistics. Fits to the analytical form discussed above are also shown, and the resulting parameters are listed in Table 2. The $H\alpha$ LF agrees with that determined from an $H\alpha$ survey of field galaxies (Gallego et al. 1995). (The faintest point, at $\log(P_{H\alpha}) = 33.5$ W, significantly deviates from the fitted LF in both studies and is therefore excluded). Applying a Schechter LF fit to the present sample gives essentially the same parameters as those derived in (Gallego et al. 1995), implying that the result here is independent from the parametric form of the LF. Considering the selection effects in the present survey (Section 2) the agreement is reassuring, and implies that $H\alpha$ -emitting objects in the faint radio population are similar to the normal $H\alpha$ -emitting galaxies in the local Universe.

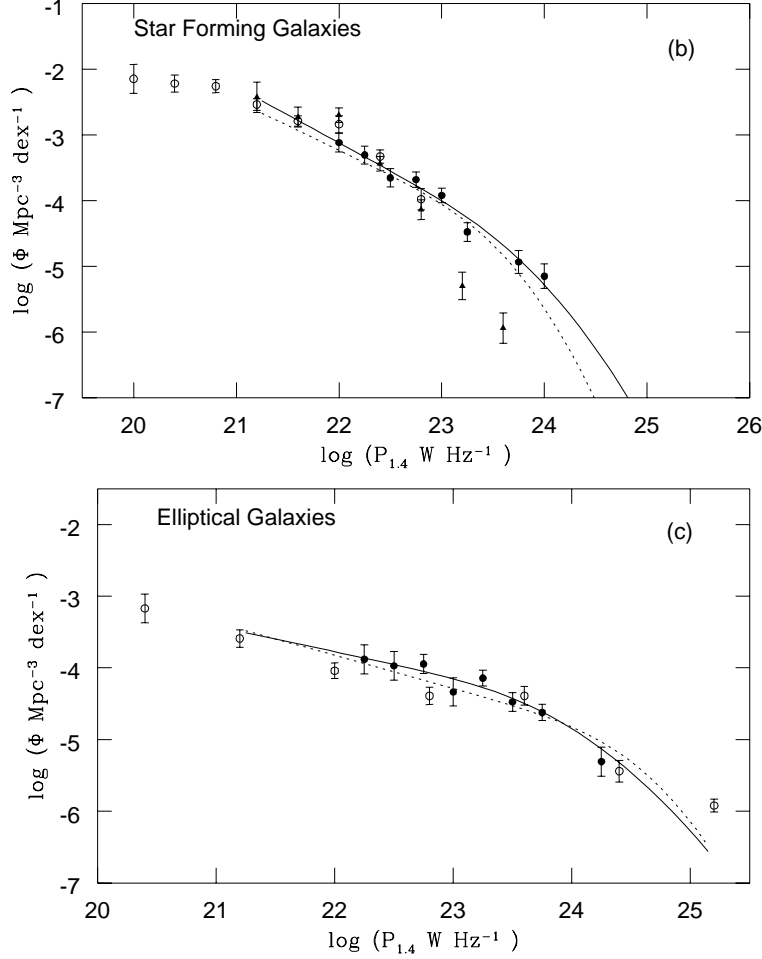


Figure 5. The 1.4 GHz luminosity functions for the faint radio population, corrected for incompleteness. Error bars are estimated assuming Poisson distribution. The curves present parametric fits to the LFs, using the function described in the text and assuming no evolution (solid lines) and luminosity evolution in the form $(1+z)^3$ (dotted lines). The LFs are estimated in the range $z < 1$ and correspond to (b) star-forming galaxies here (filled circles) compared to the spiral/star-forming (open circles) and starburst (filled triangles) galaxies from Condon (1984) and (c) elliptical galaxies from this study (solid circles) compared with ellipticals from Sadler et al. (1990) (open circles).

The slope of the faint-end of the radio LF increases from $\alpha = 1.35$ for ellipticals (Fig. 5c) to $\alpha = 1.85$ for the star-forming population (Fig. 5b). A similar result was also reported by Condon (1989). It implies that in the redshift range $0 < z < 1$ and at modest radio powers ($P_{1.4} \lesssim 10^{23} \text{ W/Hz}$), there is an abundance of star-forming galaxies compared to ellipticals. At the median redshift of our survey, $z \approx 0.3$, galaxies with $P_{1.4} \approx 10^{23} \text{ W Hz}^{-1}$ have $S_{1.4} \approx 0.2 \text{ mJy}$, and most of them have optical counterparts which will have been detected optically at a limit of $R \approx 22$. Thus, we may conclude that for the optically identified part of the sub-mJy population, the number of star-forming “IRAS-type” galaxies exceeds the number of ellipticals. Further observations of samples which are complete to known radio and optical limits would be of great value in elucidating the connection between the shape of

Table 1. Parameters of the analytical fits to the 1.4 GHz luminosity functions and the $\langle V/V_{max} \rangle$ estimates. The results are presented for all the faint radio sources in the present survey and for the starforming and elliptical sub-classes. Two different cases, assuming no evolution and luminosity evolution in the form $P_{1.4}(z) = P_{1.4}(0)(1+z)^3$ are considered.

	n	$\langle V/V_{max} \rangle$	$P_{1.4}^*$ W Hz $^{-1}$	α	σ	$C_{1.4}^*$ Mpc $^{-3}$
All types	192	0.45	$(9.59^{+2}_{-2}) \times 10^{22}$	$1.58^{+0.12}_{-0.08}$	$0.80^{+0.10}_{-0.10}$	$(2.63^{+0.40}_{-0.50}) \times 10^{-4}$
Starforming	75	0.45	$(1.18^{+0.50}_{-0.23}) \times 10^{23}$	$1.85^{+0.15}_{-0.10}$	$0.67^{+0.13}_{-0.15}$	$(9.28^{+2}_{-2}) \times 10^{-5}$
Ellipticals	63	0.42	$(1.16^{+0.35}_{-0.36}) \times 10^{23}$	$1.35^{+0.25}_{-0.20}$	$0.75^{+0.10}_{-0.15}$	$(7.15^{+2}_{-2}) \times 10^{-5}$
Luminosity Evolution						
	n	$\langle V/V_{max} \rangle$	$P_{1.4}^*$ W Hz $^{-1}$	α	σ	$C_{1.4}^*$ Mpc $^{-3}$
All types	192	0.45	$(5^{+1}_{-1}) \times 10^{23}$	$1.78^{+0.05}_{-0.10}$	$0.47^{+0.33}_{-0.10}$	$(6^{+1.5}_{-1}) \times 10^{-5}$
Starforming	75	0.45	$(1.05^{+0.80}_{-0.20}) \times 10^{23}$	$1.75^{+0.15}_{-0.10}$	$0.50^{+0.30}_{-0.05}$	$(1^{+0.80}_{-0.20}) \times 10^{-4}$
Ellipticals	63	0.42	$(1^{+1}_{-0.2}) \times 10^{24}$	$1.46^{+0.20}_{-0.05}$	$0.50^{+0.10}_{-0.20}$	$(1.8^{+1}_{-0.20}) \times 10^{-5}$

Table 2. Parameters of the analytical fits to the H α luminosity functions and the $\langle V/V_{max} \rangle$ estimates. The results are presented for all the faint radio sources in the present survey and for the starforming population

	n	$\langle V/V_{max} \rangle$	$P_{H\alpha}^*$ W	α	σ	$C_{H\alpha}^*$ Mpc $^{-3}$
All types	132	0.47	$(0.45^{+0.03}_{-0.05}) \times 10^{35}$	$1.05^{+0.05}_{-0.07}$	$0.33^{+0.03}_{-0.05}$	$(4.18^{+0.40}_{-0.7}) \times 10^{-4}$
Starforming	75	0.45	$(0.28^{+0.01}_{-0.03}) \times 10^{35}$	$0.89^{+0.02}_{-0.02}$	$0.40^{+0.01}_{-0.04}$	$(4.62^{+0.40}_{-0.70}) \times 10^{-4}$

the LF for $z \lesssim 1$, possible evolutionary effects, and the observed source count distributions including objects which have not yet been optically identified.

There are seven detections of elliptical galaxies with H α in the present survey. It is important to note that sub-mJy radio sources classified as elliptical galaxies have rest frame $V - R$ colours close to those of ‘normal’ ellipticals ($V - R \approx 0.6$) and follow their $V - R$ colour-magnitude relation (Georgakakis et al. 1998). Therefore, although the radio emission may be from an AGN, there is little evidence of AGN emission in the optical continuum. It is not excluded that both the radio and the H α emission from these objects is related at least in part to star-forming activity at a level too weak to dominate the optical continuum colours.

3.3 Luminosity density distributions and star formation rates

The main source of uncertainty in converting the observed luminosity to star formation rate (SFR) is the dependence of the calibration on a number of poorly known parameters, including the initial mass function and the history of star formation prior to the epoch

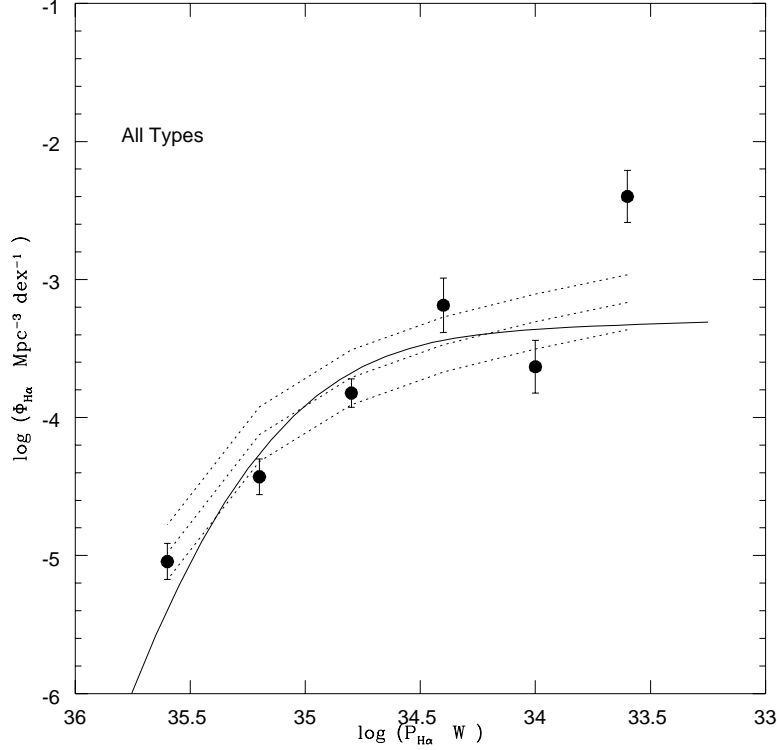


Figure 6. The $H\alpha$ luminosity function with a parametric fit (solid lines) for all galaxies with $H\alpha$ detection in the radio survey. This is compared with the $H\alpha$ luminosity function from an $H\alpha$ -selected sample of star forming galaxies (Gallego et al. 1995) - (dotted lines).

of measurement. Differences of at least a factor of 2 exist between different estimates of SFR due to these parameters. To overcome this problem, we define the luminosity density distribution as

$$\mathcal{L}_k(P_k) = P_k \Phi_k(P_k),$$

where $k = 1, 2$ correspond respectively to 1.4 GHz and $H\alpha$ wavelengths. This distribution provides an intermediate step between the luminosity function and the star formation rate density and can be determined without the uncertainties due to calibration of star formation rate *versus* the luminosity.

Luminosity density distributions for the radio and $H\alpha$ samples are presented in Figures 7(a) and 7(b) respectively. The integral of these luminosity density distributions give the luminosity densities, \mathcal{L}_k , for the radio and $H\alpha$ samples, as listed in Table 2. The 1.4 GHz luminosity density for the star-forming population in the range $z \lesssim 1$ ($2.63 \times 10^{19} \text{ W Hz}^{-1} \text{ Mpc}^{-3}$) is in excellent agreement with the value of $2 \times 10^{19} \text{ W Hz}^{-1} \text{ Mpc}^{-3}$ determined by Condon (1989). Also, the $H\alpha$ luminosity density for the faint radio sources in this study

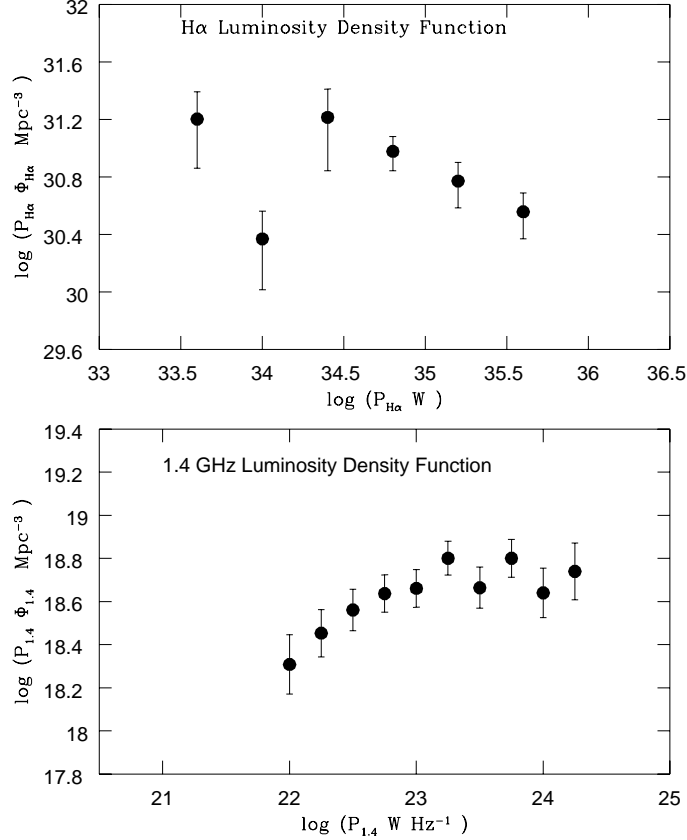


Figure 7. The luminosity density distributions, $P_k \Phi(P_k)$, for the 1.4 GHz radio (a) and H α (b) surveys of faint radio sources. The error bars correspond to Poissonian uncertainties.

($0.91 \times 10^{32} \text{ W Mpc}^{-3}$) is consistent with the value of $\mathcal{L}_{H\alpha} = 1.26 \times 10^{32} \text{ W Mpc}^{-3}$ determined by Gallego et al. (1995), using an H α selected low-dispersion objective-prism survey of nearby ($z < 0.045$) galaxies. Considering that these surveys are entirely independent and have different selection criteria, the agreement is remarkably good.

The relative contribution from the star-forming and elliptical populations to the radio luminosity densities are shown as a function of their radio luminosity in Fig. 8. The star-forming population dominates the radio luminosity density at $P_{1.4} \simeq 10^{22} - 10^{23} \text{ W Hz}^{-1}$ while the ellipticals (possibly with AGN activity) contribute significantly at $P_{1.4} \gtrsim 10^{23} \text{ W Hz}^{-1}$. The implication of this result is that the main contribution to the radio luminosity density at high redshifts, using flux-limited radio surveys, is from the elliptical/AGN population (because these dominate the bright-end of the radio LF)-(Fig. 8).

The luminosity density distribution, $\mathcal{L}_k(P_k)$, can be converted to the star formation rate density, SFR_k , using model-dependent conversion factors corresponding to

$$\text{SFR}_{1.4} = \frac{\mathcal{L}_{1.4}}{8.07 \times 10^{20} \text{ W Hz}^{-1}} \text{ M}_{\odot} \text{ yr}^{-1}$$

[h]

Table 3. Integrated luminosity densities and star formation rate densities for the faint radio population. The SFR densities are derived from both the 1.4 GHz and the H α measurements. The results are presented for different types of objects in the sample.

	z	$n_{1.4}$	$\log(\mathcal{L}_{1.4})$ W Hz $^{-1}$ Mpc $^{-3}$	$\log((SFR)_{1.4})$ M $_{\odot}$ yr $^{-1}$ Mpc $^{-3}$	$n_{H\alpha}$	$\log(\mathcal{L}_{H\alpha})$ W	$\log((SFR)_{H\alpha})$ M $_{\odot}$ yr $^{-1}$ Mpc $^{-3}$
All Types	0 – 0.3	97	19.47 $^{+0.05}_{-0.06}$		72	31.91 $^{+0.12}_{-0.16}$	–1.55
	0.3 – 1	95	19.63 $^{+0.05}_{-0.06}$		60	30.96 $^{+0.08}_{-0.09}$	–2.50
	0 – 1	192	19.86 $^{+0.04}_{-0.04}$		132	31.96 $^{+0.11}_{-0.14}$	–1.50
Starforming	0 – 0.3	52	19.27 $^{+0.07}_{-0.08}$	–1.64			
	0.3 – 1	23	18.88 $^{+0.09}_{-0.11}$	–2.02			
	0 – 1	75	19.42 $^{+0.06}_{-0.07}$	–1.49	75	31.92 $^{+0.11}_{-0.11}$	–1.53
Ellipticals	0 – 0.3	26	18.79 $^{+0.08}_{-0.10}$				
	0.3 – 1	37	19.23 $^{+0.08}_{-0.10}$				
	0 – 1	63	19.36 $^{+0.06}_{-0.08}$		7	29.20 $^{+0.16}_{-0.25}$	–4.26

after Condon (1992) and

$$SFR_{\alpha} = \frac{\mathcal{L}_{H\alpha}}{2.85 \times 10^{33} \text{W}} \text{ M}_{\odot} \text{yr}^{-1}$$

after Gallego et al. (1995). The conversion factors and hence the resulting SFR densities have been adjusted to an initial mass function $\psi(M) \propto M^{-2.35}$ for $0.1 < M/M_{\odot} < 100$. Intercomparison between SFR_{α} and $SFR_{1.4}$ relies on the validity of the calibration of the 1.4 GHz luminosity of galaxies in terms of their past supernova rate (Condon & Yin 1990). As discussed by Cram et al. (1998) and Cram (1998), this calibration is quite uncertain. Using the above calibrations, the global SFR densities are estimated and listed in Table 2. The values of $SFR_{1.4}$ are derived from the radio luminosity densities of galaxies with optical spectral morphologies classified as star forming, while the values of SFR_{α} are based on the H α luminosity density for all galaxies with H α detected.

We find $SFR_{1.4} = 0.032 \text{ M}_{\odot} \text{yr}^{-1} \text{ Mpc}^{-3}$ for $z < 1$, is close to the value estimated from optical studies (Madau et al. 1996; Hogg et al. 1998). Also, it is similar to the value $SFR_{\alpha} = 0.031 \text{ M}_{\odot} \text{yr}^{-1} \text{ Mpc}^{-3}$ we find for galaxies in the same redshift range. There is a rather large difference between $SFR_{1.4}$ and SFR_{α} for the range $0.3 < z < 1$. This may be due to a combination of several effects, including small-number statistics, greater extinction at higher redshift and errors arising from the use of [OII]3727 as a proxy for H α .

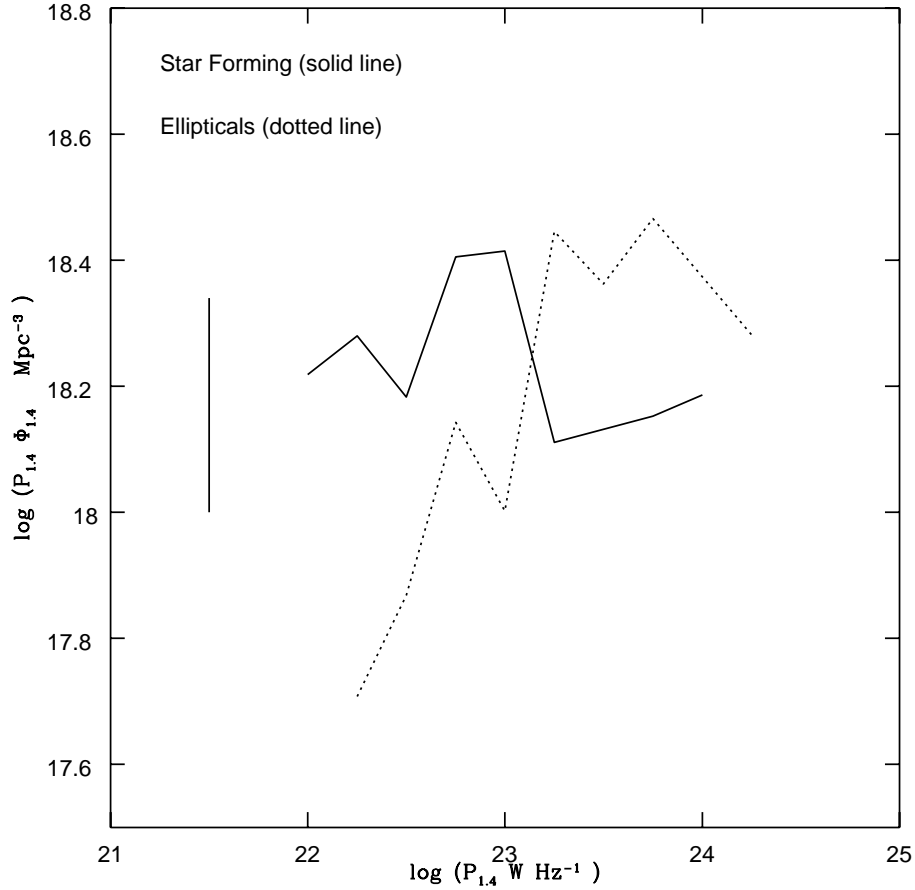


Figure 8. The 1.4 GHz luminosity density distributions, $P_{1.4} \Phi(P_{1.4})$, for the star forming population (solid line) and elliptical galaxies (dotted line).

The value of SFR_α derived from our estimate of the $\text{H}\alpha$ luminosity density can be compared directly with that of Gallego et al. (1995) provided that we ensure that the conversion factors refer to the same initial mass function. Our value, $\text{SFR}_\alpha = 0.032 \text{ M}_\odot \text{ yr}^{-1} \text{ Mpc}^{-3}$ for $z < 1$ is close to that value of $0.043 \text{ M}_\odot \text{ yr}^{-1} \text{ Mpc}^{-3}$ found by Gallego et al. (1995) when adjusted to the same IMF. Our $\text{H}\alpha$ sample is dominated by star-forming (disk) galaxies, implying that the star-forming radio sources are similar to those selected at optical (i.e. $\text{H}\alpha$) wavelengths.

It is worth noting that the Gallego et al. (1995) sample only covers galaxies in the range $z < 0.045$. Considering this and the results in Table 2, we have not been able to establish evidence of cosmic evolution in the global star formation rate (Table 2), despite the fact that some of the radio-selected star-forming galaxies lie at redshifts $z > 0.5$ where the global SFR might exceed the local rate by a factor of the order of $10^{0.5}$ (Madau et al. 1996).

This conclusion reflects the statistical uncertainty of our small sample size and is consistent with other similar investigations (Tresse and Maddox 1998).

4 CONCLUSION

A sample of over 1000 faint radio sources, selected at 1.4 GHz and ‘complete’ (to 50%) to a flux density limit of ≈ 0.2 mJy, is used for this study. Complete R -band optical photometry is carried out to $R = 22.5$, with the optical spectroscopy successfully attempted for over 225 galaxies selected at random from the radio sources with optical counterparts brighter than $R = 21.5$. The spectra have been used to derive redshifts and to make spectroscopic classifications of the optical galaxies into elliptical, star-forming and Seyfert classes. The statistical analysis is carried out on the ‘complete’ radio survey and the faint radio sources showing $H\alpha$ emissions in their spectra. Conclusions from this study are summarised as follows:

(i) Taking into account the various selection effects which define the two-wavelength sample, we have derived the radio and $H\alpha$ luminosity functions for both starforming and elliptical populations in the interval $0 < z < 1$. The LFs are well fitted to models, assuming no evolution or luminosity evolution in the form $P_{1.4}(z) = P_{1.4}(0)(1 + z)^3$. Therefore, the faint radio sources are not affected by luminosity evolution at the median redshift ($z < 0.3$) of the present sample.

Both the radio and $H\alpha$ LFs agree closely with their counterparts obtained from studies of nearby ($z \lesssim 0.05$) galaxies.

(ii) The radio (1.4 GHz) LF of the star-forming population shows a steeper faint-end slope than its counterpart for the ellipticals. This implies that there is a large population of faint radio sources undergoing star formation at $z \sim 0.3$, corresponding to the median redshift of the present sample.

(iii) The luminosity densities are estimated and used to derive the star formation rate densities for both the radio and $H\alpha$ data. These give a similar SFR density of $0.032 \text{ M}_{\odot} \text{ yr}^{-1} \text{ Mpc}^{-3}$ at $z \sim 0.3$. Moreover, The SFR density estimated here is close to those found from optical studies. This indicates the efficiency of radio observations in selecting the star-forming population, free from biases induced by dust.

(iv) The SFR density based on the $H\alpha$ data, due to the radio sources in the range $0 < z < 1$, is $0.032 \text{ M}_{\odot} \text{ yr}^{-1} \text{ Mpc}^{-3}$ which is close to the local value of $0.042 \text{ M}_{\odot} \text{ yr}^{-1} \text{ Mpc}^{-3}$ derived

by Gallego et al. (1995). Assuming no luminosity evolution in the faint radio population, this suggests that the star-forming behaviour of faint radio sources is similar to that of star-forming galaxies selected at optical wavelengths.

The Australia Telescope is funded by the Commonwealth of Australia for operation as a National Facility managed by CSIRO. LC and AH acknowledge financial support from the Australian Research Council and the Science Foundation for Physics within the University of Sydney. We thank Drs Carole Jackson and Elaine Sadler for several helpful discussions.

REFERENCES

- Baum S. A., Heckman T., 1989, *ApJ*, 336, 681
- Benn C. R., Rowan–Robinson M., McMahon R. G., Broadhurst T. J., Lawrence A., 1993, *MNRAS*, 263, 98
- Blain A. W., Smail I., Ivison R., J., Kneib J.-P., 1998, *MNRAS* (in press)
- Bruzual A. G., Charlot S., 1993, *ApJ*, 405, 538
- Condon J. J., Condon M. A., Gisler G., Puschell J. J., 1982, *ApJ*, 252, 102
- Condon J. J., 1984, *ApJ*, 287, 461
- Condon J. J., 1989, *ApJ*, 338, 13
- Condon J. J., 1992, *ARA&A*, 30, 575
- Condon J. J., Yin Q. F., 1990, *ApJ*, 357, 97
- Cram L. E., 1998, *ApJ*, 506, L85
- Cram L. E., Hopkins A. M., Mobasher B. M., Rowan-Robinson M. R., 1998, *ApJ*, 507, 155
- Danese L., De Zotti G., Franceschini A., Toffolatti L., 1987, *ApJ*, 318, L15
- Fomalont E. B., Kellerman K. I., Wall J. V., Weistrop D., 1984, *Science*, 225, 23
- Franceschini A., Danese L., De Zotti G., Toffolatti L., 1988, *MNRAS*, 233, 157
- Franceschini A., Mazzei P., De Zotti G., Danese L., 1994, *ApJ*, 427, 140
- Gallego J., Zamamoro J., Aragón-Salamanca A., Rego M., 1995, *ApJ*, 455, L1
- Georgakakis A., Mobasher B., Hopkins A., Cram L., Lidman C., Rowan-Robinson M., 1998, *MNRAS* accepted astro-ph 9903016
- Hammer F., Crampton D., Lilly S., le Fèvre O., Kenet T., 1995, *MNRAS*, 276, 1085
- Hine R. G., Longair M. S., 1979, *MNRAS*, 188, 111
- Hopkins A. M., Mobasher B., Cram L., Rowan-Robinson M., 1998a, *MNRAS*, 296, 839
- Hopkins A., Cram L., Mobasher B., Georgakakis A. 1999, in “Looking Deep in the South” (in press)
- Kauffmann G., Charlot S. 1998, *MNRAS*, 297, L23
- Kawara et al. 1998, *A & A* 336, L9.
- Kennicutt, R. C., 1992, *ApJ*, 388, 310
- Kron R. G., Koo D. C., Windhorst R. A., 1985, *A&A*, 146, 38
- Lilly, S. J., Le Fevre, O., Hammer, F., Crampton D., 1996, *Ap.J.* 460, L1
- Lonsdale C. L., Hacking P. B., Conrow T. P., Rowan-Robinson M., 1990, *ApJ*, 358, 60
- Madau P., Ferguson H. C., Dickinson M. E., Giavalisco M., Steidel C. C., Fruchter A., 1996, *MNRAS*, 283, 1388
- Mitchell K. J., Condon J. J., 1985, *AJ*, 90, 1957
- Rowan-Robinson M., Benn C. R., Lawrence A., McMahon R. G., Broadhurst T. J., 1993, *MNRAS*, 263, 123
- Rowan-Robinson M. R., et al. 1997, *MNRAS*, 289, 490
- Sadler E., Jenkins C., Kotanyi C., 1989, *MNRAS*, 240, 591

- Sanders D. B., Mirabel I. F., 1996, ARA&A, 34, 749
- Saunders W., Rowan-Robinson M., Lawrence A., Efstathiou G., Kaiser N., Ellis R. S., Frenk C. S., 1990, MNRAS, 242, 318
- Thuan T. X., Condon J. J., 1987, ApJ, 322, L9
- Tresse L., Maddox S. J., 1998, ApJ, 495, 691
- Wall J. V., Jackson C. A., 1997, MNRAS, 290, L17
- Windhorst R. A., van Heerde G. M., Katgert P., 1984, A&AS, 58, 1
- Windhorst R. A., Miley G. K., Owen F. N., Kron R. G., Koo D. C., 1985, ApJ, 289, 494